Am J Transl Res 2017;9(2):289-300
www.ajtr.org /ISSN:1943-8141/AJTR0039018

Original Article

miR-590-3p mediates the protective effect of curcumin on injured endothelial cells induced by angiotensin II

Tian Wu[1], Yuanyuan Xiang[1], Yu Lv[1], Dai Li[2], Lijin Yu[1], Ren Guo[1]

[1]Department of Pharmacy, The Third Xiangya Hospital, Central South University, Changsha, Hunan, China; [2]Department of Pharmacy, Xiangya Hospital, Central South University, Changsha, Hunan, China

Received August 29, 2016; Accepted January 31, 2017; Epub February 15, 2017; Published February 28, 2017

Abstract: Curcumin (Cur) has multiple pharmacological effects including antitumor, anti-inflammatory, antioxidant and cardiovascular protective effects. This research aims to further explore whether the cardiovascular protective effects of Cur are mediated by the miR-590-3p/CD40 pathway. Endothelial cells (ECs) were cultivated with 10^{-7} mol/L angiotensin II (Ang II) to establish a damage model. Real-time PCR was used to determine the expression of CD40 and eNOS mRNA on ECs. The protein expressions of CD40 and eNOS were detected by Western blot analysis. The intracellular activities of SOD, CAT and MDA level were determined by corresponding detection kits, and the level of reactive oxygen species (ROS) in ECs was measured by ROS assay kit. Ang II increased both the mRNA and protein level of CD40, while it down-regulated the expression of eNOS at mRNA and protein level. These observations were accompanied by decreased activities of SOD and CAT with increased levels of intracellular MDA and ROS. Cur and miR-590-3p mimics inhibited the expressions of CD40 mRNA and protein induced by Ang II and alleviated the intracellular oxidative stress seen with increased levels of eNOS. However, these beneficial effects caused by Cur were partially reversed in the presence of miR-590-3p inhibitors. Our results indicate miR-590-3p is involved in the anti-inflammatory effects of Cur in ECs damaged by Ang II.

Keywords: Curcumin, Ang II, CD40, eNOS, miR-590-3p, ROS

Introduction

The endothelium, a thin layer covering the lining of blood vessels, maintains the permeability of the vessel wall and vascular homeostasis. Accumulating evidence has shown that endothelial dysfunction and the impaired production or activities of nitric oxide (NO) are considered markers for atherosclerosis (AS) [1, 2]. It is reported that enhanced levels of oxidative stress lead to eNOS uncoupling and inhibited NOS activity, which finally cause endothelial dysfunction in various cardiovascular diseases through the eNOS/ADMA/DDAH pathway [3, 4]. The function of CD40/CD40 ligand (CD40L) in AS has been well studied. The CD40/CD40L system plays a crucial role in the pathophysiology of AS via up-regulating the expression of proinflammatory and prothrombotic genes [5]. Additionally, the CD40/CD40L signaling pathway may modulate endothelial reactive oxygen species (ROS) generation [6]. Hausding, M. and his colleagues have reported that CD40L was associated with vascular inflammation, oxidative stress and a pro-thrombotic state induced by angiotensin II in an animal model [7]. Increased levels of sCD40L also resulted in an impaired anti-platelet function of peripheral blood angiogenic outgrowth cells through elevated production of ROS [8].

miRNAs are a group of small non-coding RNAs approximately 22 nucleotides in length, which usually act as a negative regulator by binding the 3'-untranslated region (UTR) of their target mRNAs [9]. Emerging studies have demonstrated the role of the miR-590 family, a vital group of miRNAs involved in the regulation of cell differentiation, in the pathological processes of many diseases. Pang H and his colleagues reported that miR-590-3p suppressed epithelial mesenchymal transition (EMT) and metastasis of glioblastoma multiforme (GBM) cells through inhibiting the expression of Zinc finger E-box-binding homeobox (ZEB) 1 and ZEB2 [10]. Recent studies focused on the cardiovascular protective effects of miR-590 have suggested that mR-590 could protect endothelial

cells (ECs) from ox-LDL and angiotensin II (Ang II)-induced damage in the LOX-1-ROS-p38MAPK-NF-κB signaling cascade and the p53-Bcl-2/Bax-caspase-3 signaling pathway [11-13]. However, to date, there is no research having reported on the possible relationship between miR-590 and CD40.

Curcumin (Cur), a polyphenolic compound extracted from Curcuma longa L., has multiple pharmacological activities including antitumor, anti-inflammatory, antioxidant and cardiovascular protective effects [14-17]. Cur has a melting point of 183°C, a molecular formula of $C_{21}H_{20}O_6$ and molecular weight of 368.37. Cur is practically insoluble in water but, easily soluble in ethanol, alkali, acetone and chloroform [18-20]. To further elucidate the mechanism of cardiovascular protection of Cur, we first established the Ang II-induced injured ECs model and investigated whether the protective role of Cur depended on a miR-590/CD40 mediated pathway.

Materials and methods

Drugs and reagents

Cur was purchased from National Institutes for Biological Products Control (China). The purity of Cur was over 99% detected by high performance liquid chromatography (HPLC) and nuclear magnetic resonance spectroscopy (H-NMR). Ang II and dimethyl sulfoxide were purchased from Sigma (St. Louis, USA). DMEM was purchased from Gibco (New York, USA). Fetal Bovine Serum (FBS) was purchased from Hao Yang (Tianjin, China). Reverse transcription and Real-time PCR Kits were purchased from TAKARA (Dalian, China). SOD, CAT and MDA Kits were purchased from Jiancheng (Nanjing, China). ROS Detection Kit and BCA Protein Assay Kit were purchased from Beyotime (Jiangsu, China). Goat anti-CD40 and anti-eNOS antibodies were purchased from Millipore. HRP-labeled goat anti-rabbit antibody was purchased from MBI.

Cell culture

ECs (HUVEC-12) were cultured in 10% FBS DMEM medium and grown to 80% in the incubator with 5% CO_2 at 37°C. Before drug administration, ECs were washed with phosphate buffered saline (PBS) and rendered quiescent in 1% serum DMEM for 24 h. Cells were divided into the following 5 groups: (1) Control: Control group; (2) Ang II: 10^{-7} mol/L Ang II treated group; (3) Ang II+Cur: pretreated cells with 10^{-5} mol/L Cur before 10^{-7} mol/L Ang II; (4) Ang II+miR-590-3p mimic: pretreated cells with 50 nmol/L miR-590-3p mimic before 10^{-7} mol/L Ang II; and (5) Ang II+Cur+miR-590 inhibitor: pretreated cells with 10^{-5} mol/L Cur and 100 nmol/L miR-590-3p inhibitor before 10^{-7} mol/L Ang II.

MTT assay

Resuspended ECs were plated in the 96-well plate at a density of $1*10^5$ cells/mL, to each well 200 μL of the cell suspension was added. PBS was added to the 96-well plate as a sealant. Cells were incubated with 5% CO_2 at 37°C. After attachment growth, the supernatant was discarded, and fresh low glucose DMEM medium containing 1% FBS was added for cell synchronization. After synchronizing 12 h, 100 μL of medium containing corresponding concentrations of Ang II was added according to our established groups and incubated with 5% CO_2 at 37°C. We then took out the 96-well plate at 12 h, 24 h, and 48 h, respectively, (away from light), added 10 μL MTT solution (5 mg/mL) and then incubated with 5% CO_2 at 37°C for 4 h. Medium was discarded, 200 μL DMSO was added and the plate was shaken for 15 min to make sure blue-violet crystals were completely dissolved. Then, the sample was quantified at 490 nm using the spectrophotometer. The cell inhibition rate/%=(absorbance value of the control group - absorbance value of each group)/control group absorbance value.

SOD, CAT and MDA detection

Cell disruption was acquired by repeated freezing and thawing. Cell solution was then centrifuged at 3000 rpm for 10 min, and the supernatant was collected. BCA Protein Assay Kit was used for measuring the contents of SOD, CAT and MDA.

ROS detection

Cells were seeded at a density of $1*10^5$ cells/mL in the 96-well plate. Cells were washed three times by PBS after drug treatment, and medium containing 10 μmol/L DCFH-DA was added in each well and incubated with 5% CO_2 at 37°C 20 min (away from light). Cells were washed three times by serum-free medium,

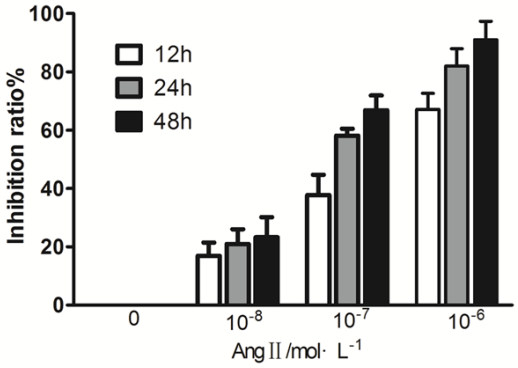

Figure 1. Effects of different concentrations and incubation times of Ang II on ECs. The descriptive results are expressed as the mean ± SD, n=6.

and the fluorescence intensity was determined by fluorescence spectroscopy (excitation wavelength of 488 nm, emission wavelength of 525 nm).

Real-time PCR analysis

Target and reference gene primers were designed by Prime Premier 5.0 software. Primers were synthesized by Shanghai Sangon Biological Engineering Technology and Service Co., Ltd. CD40: forward primer, 5'-GCAGGCACAAACAAGACTGA-3', reverse primer, 5'-TCGTCGGGAAAATTGATCTC-3'. eNOS: forward primer, 5'-GCAACCACATCAAGTATGCCACCAA-3' reverse primer, 5'-GCTGTTCCAGATTCGGAAGTCTCCT-3'. GAPDH: forward primer, 5'-CTGCACCACCAACTGCTTAG-3', reverse primer, 5'-AGGTCCACCACTGACACGTT-3'. PCR reaction parameters: initial denaturation at 95°C (10 s), denaturation at 95°C (5 s), annealing and extension at 60°C (31 s) followed by 40 cycles. All amplification reactions were performed in triplicate and the averages of the threshold cycles (Cts) were used to interpolate curves with ViiA™ 7 System SDS Software. The results were expressed as the ratio of target gene with GAPDH mRNA.

Western blotting

Exponentially growing ECs were divided into 5 groups: (1) Control: Control group; (2) Ang II: 10^{-7} mol/L Ang II treated group; (3) Ang II+Cur: pretreated cells with 10^{-5} mol/L Cur before 10^{-7} mol/L Ang II; (4) Ang II+miR-590-3p mimic: pretreated cells with 50 nmol/L miR-590-3p mimic before 10^{-7} mol/L Ang II; and (5) Ang II+Cur+miR-590 inhibitor: pretreated cells with 10^{-5} mol/L Cur and 100 nmol/L miR-590-3p inhibitor before 10^{-7} mol/L Ang II. Every group was incubated with ECs for 24 h. Cells were resuspended by PBS, and then protein was extracted. Protein samples mixed with loading buffer were degenerated at 95°C for 5 min and then naturally cooled. Samples (20 μg) were loaded in the gel, and electrophoresis (60 V integrated voltage, 120 V constant voltage) was performed. A semi-dry transfer method was used to transfer proteins from gel to membrane for 48 min. Nonfat 5% milk was used to block for 1 h, and then the diluted primary antibody was added and incubated at 4°C for 16 h. The membrane was washed, and the diluted secondary antibody was added and shaken at room temperature for 1 h. The blots were detected using the ChemiDoc XRS+ Image system (Bio-Rad, USA).

Dual luciferase reporter assay

The wild-type human CD40 3'-UTR sequence containing predicted miR-590-3p target sites and mutant 3'-UTR of CD40 were synthesized and inserted into the pGL3 control vector (Promega, USA). For the reporter assay, ECs were seeded into 24-well plates and co-transfections of CD40-3'UTR or mut-CD40-3'UTR plasmid were performed with miR-590-3p mimics or negative control. Luciferase activities were evaluated using the dual luciferase assay system (Promega, USA) after 24 h incubation.

Statistical analysis

SPSS software (Version 11.5) was used for the statistical analysis. The data were expressed as the mean ± SD. A two-tailed Student's t-test was used for the comparison of differences between two independent groups. The differences among the groups were compared using a one-way ANOVA. $P<0.05$ was considered to be statistically significant.

Results

Ang II-induced injured ECs model

We first performed the MTT assay to determine the ideal concentration and time for ECs injury by Ang II. The cell inhibition rate was significantly elevated with the increase of Ang II concentration and time course. The ideal cell inhibition

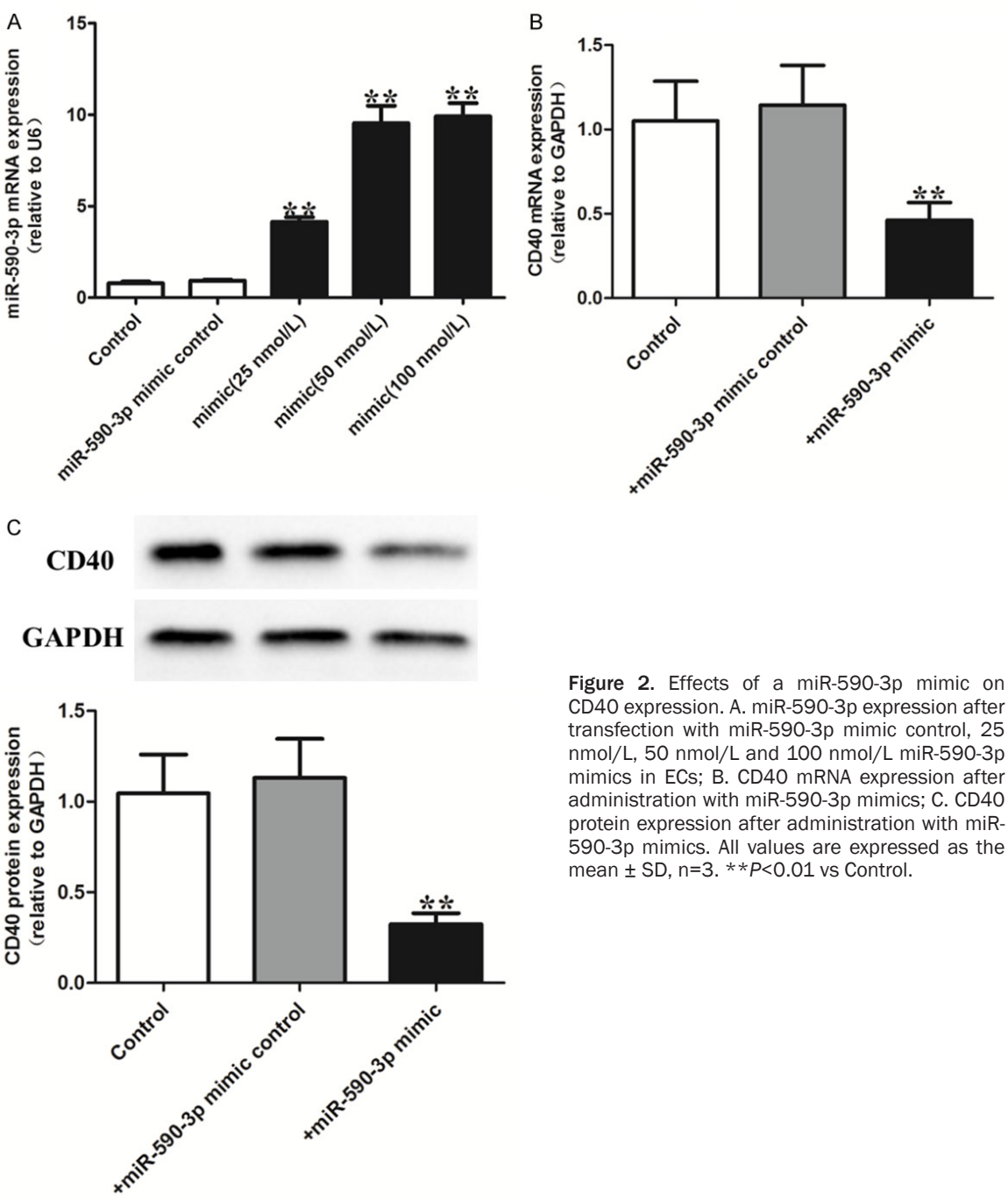

Figure 2. Effects of a miR-590-3p mimic on CD40 expression. A. miR-590-3p expression after transfection with miR-590-3p mimic control, 25 nmol/L, 50 nmol/L and 100 nmol/L miR-590-3p mimics in ECs; B. CD40 mRNA expression after administration with miR-590-3p mimics; C. CD40 protein expression after administration with miR-590-3p mimics. All values are expressed as the mean ± SD, n=3. $^{**}P<0.01$ vs Control.

rate for the experiment was approximately 60%, with an Ang II concentration of 10^{-7} mol/L for 24 h (**Figure 1**).

miR-590-3p inhibits the expression of CD40 in ECs

To test the possible effects of miR-590-3p on CD40 expression, we transfected ECs with different concentration of miR-590-3p mimics for 24 h. A dose response analysis allowed us to determine that 50 nmol/L miR-590-3p mimics led to an approximately 10-fold increase in miR-590-3p, which was appropriate for the subsequent experiment (**Figure 2A**). We then found that miR-590-3p mimics significantly inhibited CD40 expression both at the mRNA and protein levels in ECs (**Figure 2B** and **2C**). We have also confirmed that 100 nmol/L miR-590-3p inhibitor was appropriate for subsequ-

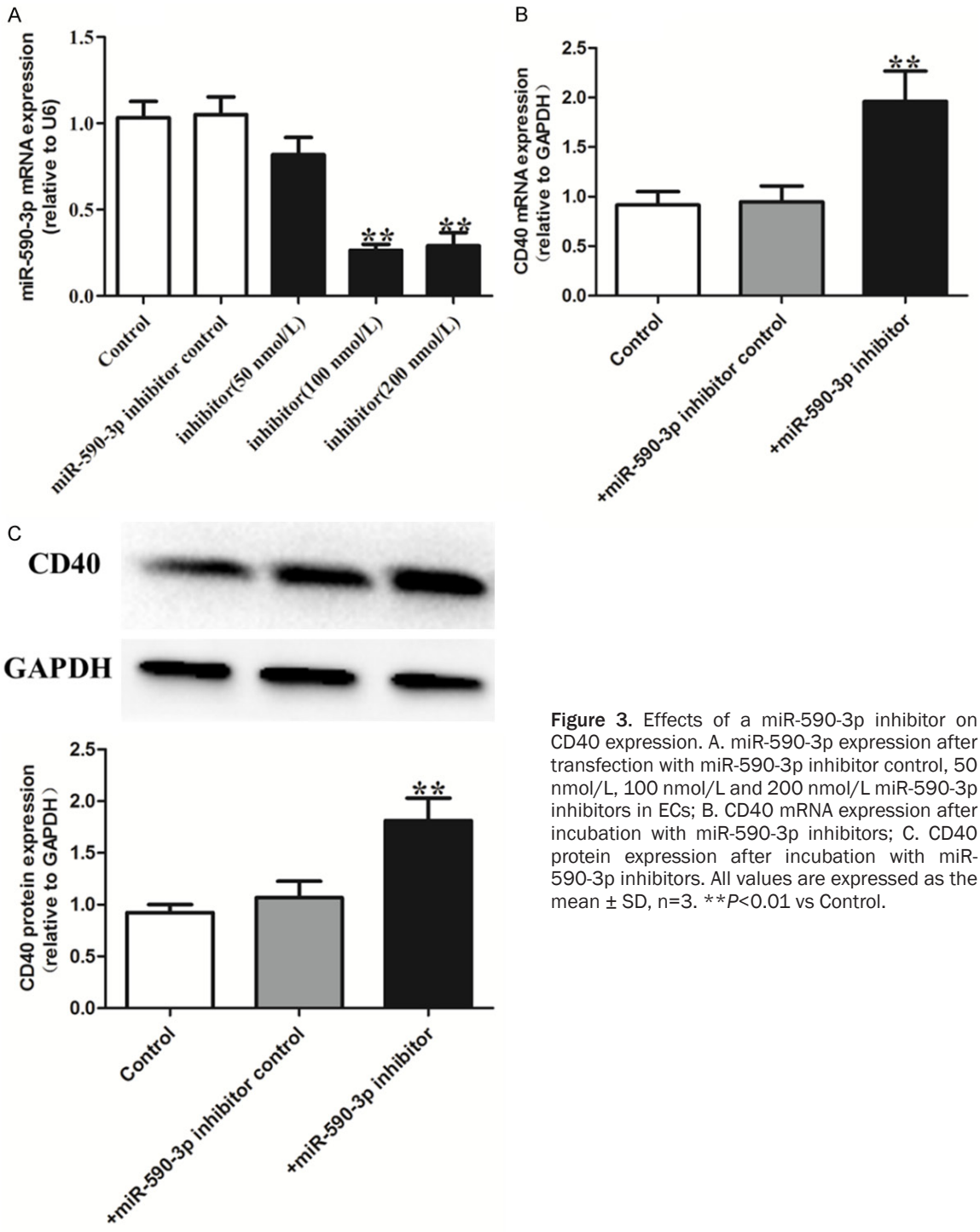

Figure 3. Effects of a miR-590-3p inhibitor on CD40 expression. A. miR-590-3p expression after transfection with miR-590-3p inhibitor control, 50 nmol/L, 100 nmol/L and 200 nmol/L miR-590-3p inhibitors in ECs; B. CD40 mRNA expression after incubation with miR-590-3p inhibitors; C. CD40 protein expression after incubation with miR-590-3p inhibitors. All values are expressed as the mean ± SD, n=3. ***P*<0.01 vs Control.

ent experiments, which can result in an approximately 5-fold decrease in miR-590-3p in ECs (**Figure 3A-C**).

miR-590-3p directly targets CD40 in ECs

We used the database of microrna.org to predict the potential target of miR-590-3p. CD40, which is known to serve a critical role in the process of inflammation, was predicted as one of the targets (**Figure 4A**). Luciferase activities assay indicated that miR-590-3p significantly suppressed the luciferase activity of wild-type but not the mutant 3'UTR of the CD40 gene in ECs (**Figure 4B**). This result suggests that CD40 is a direct target of miR-590-3p.

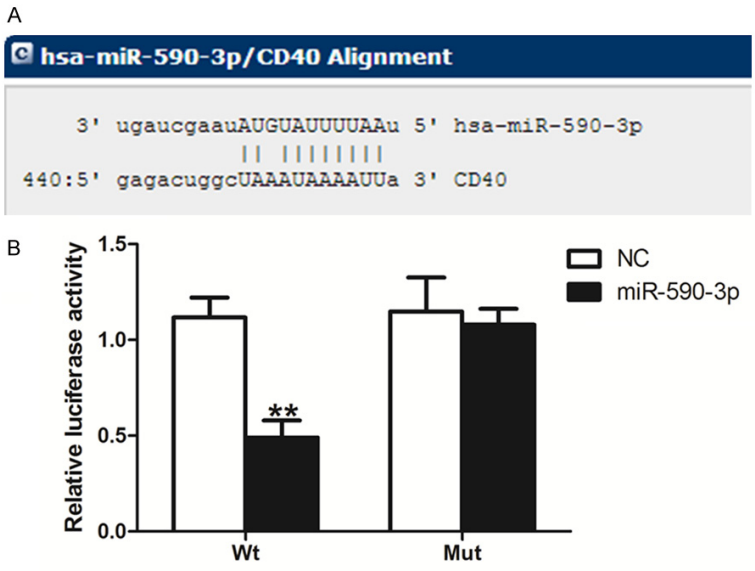

Figure 4. Dual luciferase reporter assay. A. The complementary sequence between miR-590-3p and CD40 3'UTR. B. Luciferase activities of wild-type 3'-UTR CD40 and mutant 3'-UTR CD40 constructs in ECs. All values are expressed as the mean ± SD, n=3. $^{**}P<0.01$, compared with negative control.

Table 1. Effects of Cur on lipid peroxidation and anti-oxidant enzyme activity ($\bar{x}$±s, n=3)

Group	SOD (U/mL)	CAT (U/mg protein)	MDA (nmol/mL protein)
Control	19.56±0.17	37.25±1.55	8.68±0.15
Ang II	11.08±0.54**	25.26±0.85**	12.14±0.36**
Ang II+Cur	16.72±0.96$^{\#\#}$	32.44±3.26$^{\#}$	10.09±0.80$^{\#\#}$
Ang II+miR-590	17.28±0.69$^{\#\#}$	35.18±1.62$^{\#\#}$	10.25±2.07$^{\#}$
Ang II+Cur+inhibitor	12.50±1.21$^{\&\&}$	27.24±4.24$^{\&}$	12.55±0.92$^{\&\&}$

miR-590 represents miR590-3p-mimic, inhibitor represents miR-590-3p inhibitor, $^{**}P<0.01$ *vs* Control, $^{\#}P<0.05$, $^{\#\#}P<0.01$ *vs* Ang II, $^{\&}P<0.05$, $^{\&\&}P<0.01$ *vs* Ang II+Cur.

Effects of Cur on antioxidant enzyme activity in Ang II-induced damaged cells

We detected SOD, CAT activity and MDA content to determine the cell lipid peroxidation level and the protective role of Cur. Previous research has indicated that 10^{-5} mol/L Cur showed a great efficiency on endothelial protection [21, 22]. Therefore, in the subsequent experiments of our study, we chose 10^{-5} mol/L Cur to prevent the Ang II-induced damage in ECs. Compared with the control group, the endogenous antioxidant enzyme activities of SOD and CAT were decreased, whereas the MDA content was increased in the model group. Compared with the model group, 10^{-5} mol/L Cur and 50 nmol/L miR-590-3p mimics partially restored the activities of SOD and CAT accompanied by decreased MDA content in ECs. However, pretreatment of ECs with 100 nmol/L miR-590-3p inhibitors blocked this protective effect of Cur (**Table 1**).

Effects of Cur on the ROS level induced by Ang II in ECs

Compared with the control group, the level of ROS was increased by 2.8-fold in the model group in which ECs were treated with 10^{-7} mol/L Ang II for 24 h. In comparison with the Ang II-treated group (287.32±8.63)%, the ROS level was decreased to (188.12±17.37)% ($P<0.05$), (161.38±8.96)% ($P<0.01$) after being processed by 10^{-5} mol/L Cur and 50 nmol/L miR-5903p mimics, respectively. However, pretreatment of ECs with 100 nmol/L miR-5903p inhibitors partially blocked these effects caused by Cur. Our data showed Curcan significantly inhibit the increase of intracellular ROS production induced by AngII through a miR-590-3p dependent pathway (**Figure 5**).

Effects of Cur on miR-590-3p expression in ECs

We used real-time PCR to determine the expression of miR-590-3p in different cell groups. As shown in **Figure 6**, 10^{-7} mol/L Ang II induced a remarkable decrease in miR-590-3p expression. Pretreatments of ECs with 10^{-5} mol/L Cur and 50 nmol/L miR-590-3p mimics before Ang II administration significantly reversed the expression of miR-590-3p. However, the effect of Cur on miR-590-3p expression was inhibited in the presence of the miR-590-3p inhibitor (**Figure 6**).

Effects of Cur on CD40 and eNOS expression in ECs

As mentioned above, the expression of eNOS partly reflects the endothelial function. The CD40/CD40L pathway is vital in regulating cell

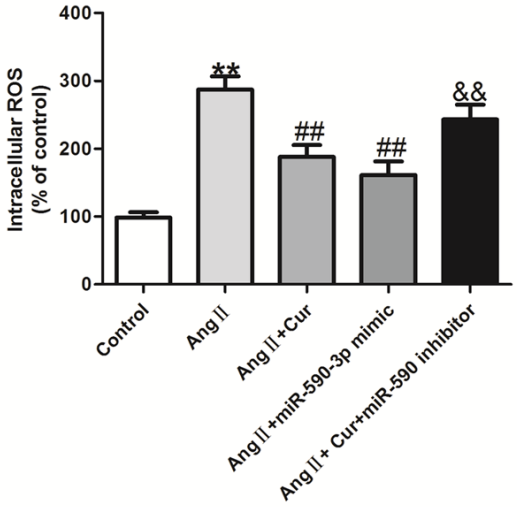

Figure 5. Effects of Cur on ROS production induced by Ang II. The descriptive results of ROS production are expressed as the mean ± SD, n=3. Control: Control group; Ang II: 10^{-7} mol/L Ang II treated group; Ang II+Cur: pretreated cells with 10^{-5} mol/L Cur before 10^{-7} mol/L Ang II; Ang II+miR-590-3p mimic: pretreated cells with 50 nmol/L miR-590-3p mimic before 10^{-7} mol/L Ang II; Ang II+Cur+miR-590 inhibitor: pretreated cells with 10^{-5} mol/L Cur and 100 nmol/L miR-590-3p inhibitor before 10^{-7} mol/L Ang II. $^{**}P$<0.01, compared with Control, $^{\#\#}P$<0.01, compared with Ang II, $^{\&\&}P$<0.01, compared with Ang II+Cur.

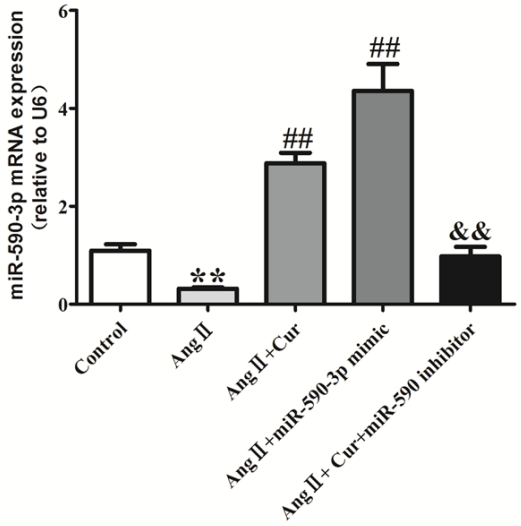

Figure 6. Effects of Cur on miR-590-3p expression in ECs. The expressions of miR-590-3p are determined by real-time PCR in different groups. Values are presented as the mean ± SD; n=3. Control: Control group; Ang II: 10^{-7} mol/L Ang II treated group; Ang II+Cur: pretreated cells with 10^{-5} mol/L Cur before 10^{-7} mol/L Ang II; Ang II+miR-590-3p mimic: pretreated cells with 50 nmol/L miR-590-3p mimic before 10^{-7} mol/L Ang II; Ang II+Cur+miR-590 inhibitor: pretreated cells with 10^{-5} mol/L Cur and 100 nmol/L miR-590-3p inhibitor before 10^{-7} mol/L Ang II. $^{**}P$<0.01, compared with Control, $^{\#\#}P$<0.01, compared with Ang II, $^{\&\&}P$<0.01, compared with Ang II+Cur.

inflammation, immunity, and oxidative stress. Therefore, in this research, we also observed the change of CD40 and eNOS expression among different groups. Compared with the control group, the expression of eNOS was decreased significantly, while CD40 expression was significantly increased at both the mRNA and protein levels in the model group. After being processed with Cur and miR-590-3p mimics, the down-regulation of eNOS was partially reversed and accompanied by a decrease of the CD40 expression induced by Ang II. These effects caused by Cur were inhibited in the presence of miR-590-3p inhibitors (**Figures 7** and **8**).

Discussion

The vascular endothelium is crucial in maintaining cardiovascular homeostasis. Endothelium dysfunction is a common pathological and physiological characteristic of a variety of cardiovascular diseases, including atherosclerosis, hypertension and diabetes. NO is an important cellular signaling molecule for cardiovascular function and its formation is catalyzed by eNOS (endothelial NOS) from L-arginine. The impairment of eNOS leads to many cardiovascular diseases including heart failure, stroke, and atherosclerosis [23-25], which may be partly due to the subsequent dysfunction of endothelium caused by the low level of NO and the abnormally increased levels of ROS induced by uncoupling of eNOS [26]. CD40, a type I transmembrane glycoprotein, belongs to the tumor necrosis factor receptor family and is expressed in a variety of cells including ECs. Additionally, many proinflammatory cytokines, such as IL-1, 3 and 4; TNF-α; and INF-γ, can stimulate the expression of CD40 [27]. CD40 is a high risk factor of atherosclerosis and may promote an inflammatory response that is associated with endothelial dysfunction and hypercoagulability [28]. Ma, Y. and his colleagues have already reported an increased level of CD40 in Ang II-treated dendritic cells combined with increased secretion of IL-12p70, IL-6, TNF-α and ROS [29]. Our team also reported

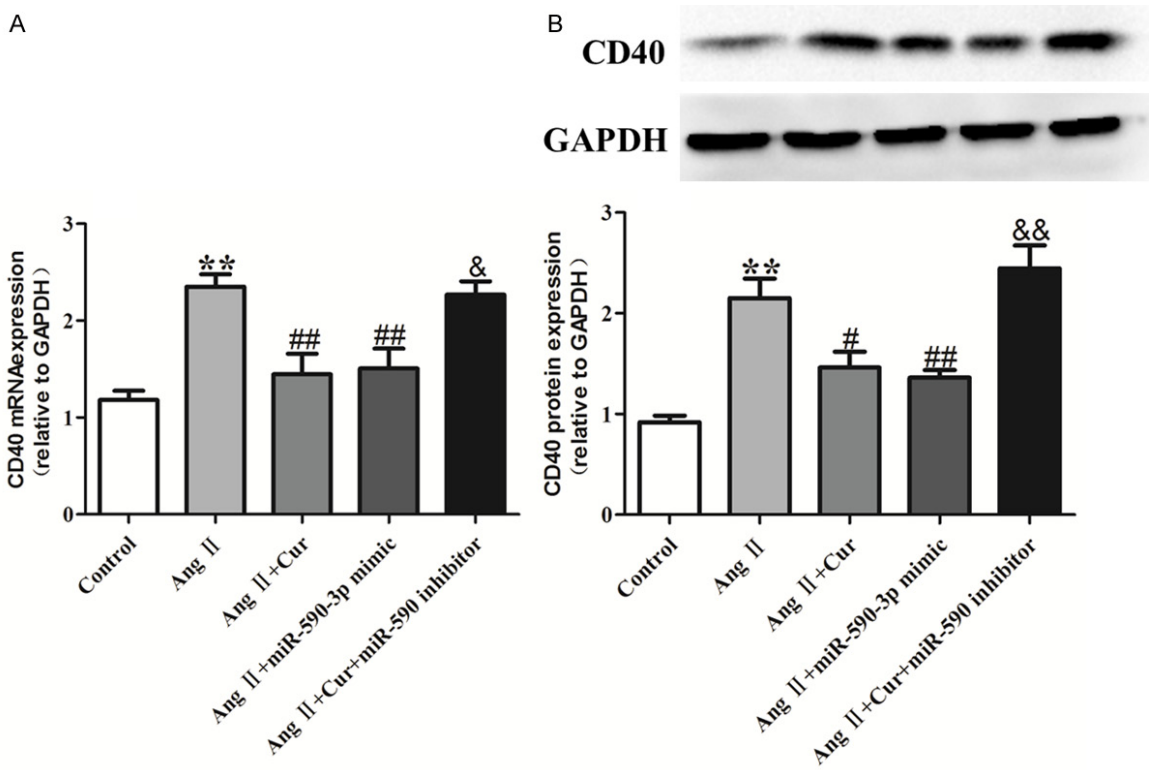

Figure 7. Effects of Cur on CD40 expression in ECs injured by Ang II. The levels of (A) CD40 mRNA expression were determined by real-time PCR; The levels of (B) CD40 protein expression were determined by Western blotting. The descriptive results of CD40 expression are expressed as the mean ± SD, n=3. Control: Control group; Ang II: 10^{-7} mol/L Ang II treated group; Ang II+Cur: pretreated cells with 10^{-5} mol/L Cur before 10^{-7} mol/L Ang II; Ang II+miR-590-3p mimic: pretreated cells with 50 nmol/L miR-590-3p mimic before 10^{-7} mol/L Ang II; Ang II+Cur+miR-590 inhibitor: pretreated cells with 10^{-5} mol/L Cur and 100 nmol/L miR-590-3p inhibitor before 10^{-7} mol/L Ang II. $^{**}P<0.01$, compared with Control, $^{\#}P<0.05$, $^{\#\#}P<0.01$, compared with Ang II, $^{\&}P<0.05$, $^{\&\&}P<0.01$, compared with Ang II+Cur.

the CD40/CD40L signaling pathway was involved in the processes of ischemic stroke and post-stroke epilepsy [30-32]. Moreover, a recent study from our group identified the anti-proliferative and anti-inflammatory effects of aspirin were partially mediated by the miR-145/CD40 pathway [33]. As we know, a certain mRNA can be regulated by several miRNAs though complete or incomplete pairing at the 3'-UTR. Sometimes, the associated miRNAs, mRNAs and transcriptional regulatory factors can form a complex regulatory network and play a critical role in the pathogenesis of many diseases. By using a bioinformatics method, we found that CD40 was also a potential target of miR-590-3p. It is therefore tempting to explore the association between CD40 and miR-590-3p. As described in the results, incubation of cells with miR-590-3p mimics significantly decreased the expression of CD40 both at mRNA and protein levels. Further, our dual luciferase reporter assay experiment also demonstrated that CD40 was a direct target of miR-590-3p.

The traditional Chinese medicine turmeric is used to treat many diseases. A wealth of scientific data suggests that Cur (the major active ingredient of turmeric) exhibits powerful antitumor, antiviral, antibacterial and antifungal properties via its regulation of various transcription factors, growth factors, protein kinases, cytokines and other enzymes. It has been reported that Cur can function as an antioxidant by inhibiting the nuclear transcription factor NF-κB. Sharma *et al.* showed that Cur significantly inhibited proliferation, antibody production and lymphokine secretion by down-regulating CD28, CD80 and up-regulating CTLA-4 and suppressed the activity of macrophages and T and B cells [34]. Duan *et al.* demonstrated that administration of Cur may attenuate ischemia-reperfusion injury in isolated perfused rat hearts [35]. Cur can also ameliorate diabetic

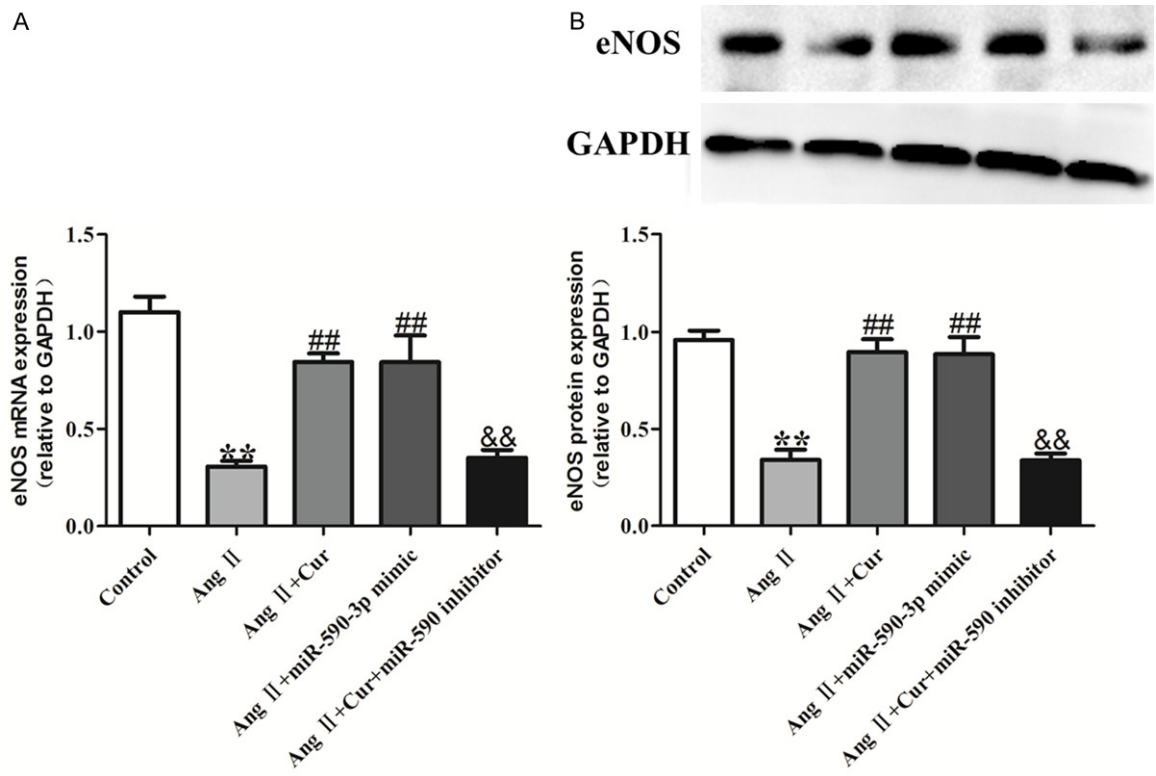

Figure 8. Effects of Cur on eNOS expression in ECs injured by Ang II. The levels of (A) eNOS mRNA expression were determined by real-time PCR; The levels of (B) eNOS protein expression were determined by Western blotting. The descriptive results of eNOS expression are expressed as the mean ± SD, n=3. Control: Control group; Ang II: 10^{-7} mol/L Ang II treated group; Ang II+Cur: pretreated cells with 10^{-5} mol/L Cur before 10^{-7} mol/L Ang II; Ang II+miR-590-3p mimic: pretreated cells with 50 nmol/L miR-590-3p mimic before 10^{-7} mol/L Ang II; Ang II+Cur+miR-590 inhibitor: pretreated cells with 10^{-5} mol/L Cur and 100 nmol/L miR-590-3p inhibitor before 10^{-7} mol/L Ang II. $^{**}P<0.01$, compared with Control, $^{\#\#}P<0.01$, compared with Ang II, $^{\&\&}P<0.01$, compared with Ang II+Cur.

cardiomyopathy in streptozotocin-induced diabetic rats [36]. Thus, Cur exerts extensive protection of the cardiovascular system. Some scientists have also investigated the association between Cur and CD40/CD40L signaling, and found that administration of Cur could inhibit the expression of CD40L and improve the permeability of coronary artery in an AS rat model as well as decrease the expression of CD40 in K562 leukemia cells [37, 38].

However, no research has addressed the possible link between the endothelial protective effects of Cur and the miR-590-3p/CD40 pathway in Ang II-treated ECs. In current study, we first established an ECs injury model by Ang II. We observed the CD40, eNOS and miR-590-3p expression, with our data showing that cells are under high level of oxidative stress in the Ang II-induced ECs injury model along with a significantly increased expression of CD40, decreased expression of eNOS and apparent suppression of miR-590-3p. The up-regulation of CD40 was inhibited in the presence of Cur or miR-590-3p mimics, and the reduction of eNOS was also partly blocked accompanied by a significant improvement in oxidative stress in ECs. It has been well documented that Ang II can induce the expression of CD40 and NF-κB signaling [39]. Activating the CD40/CD40L pathway can also induce the generation of ROS by uncoupling eNOS, resulting in ECs damage. Our results indicate that Cur protects the endothelium through inhibiting the expression of CD40 and oxidative stress levels in a miR-590-3p-dependent pathway.

It should be mentioned that more large-scale in vitro and in vivo studies are still in need to fully prove the protective mechanisms of Cur. Further pharmaceutical studies are warranted to develop Cur into a promising treatment for cardiovascular disease.

Acknowledgements

We wish to acknowledge Dr. Zhigang Ding, from the Third Xiangya Hospital, for his help to this research. This project was supported by the New Xiangya Talent Project of the Third Xiangya Hosipital of Central South University (JY201506).

Disclosure of conflict of interest

None.

Authors' contribution

Ren Guo conceived and designed the experiments; Tian Wu and Yuanyuan Xiang performed the experiments; Dai Li analyzed the data; Yu Lv and Lijin Yu contributed reagents/materials/analysis tools; Ren Guo and Dai Li wrote the paper.

Address correspondence to: Ren Guo, Department of Pharmacy, The Third Xiangya Hospital, Central South University, Changsha 410013, Hunan, China. Tel: 86-731-88618455; Fax: 86-731-88618455; E-mail: grfw2012@aliyun.com

References

[1] Stancu CS, Toma L and Sima AV. Dual role of lipoproteins in endothelial cell dysfunction in atherosclerosis. Cell Tissue Res 2012; 349: 433-446.

[2] Rozanski A, Blumenthal JA and Kaplan J. Impact of psychological factors on the pathogenesis of cardiovascular disease and implications for therapy. Circulation 1999; 99: 2192-2217.

[3] Novella S, Laguna-Fernandez A, Lazaro-Franco M, Sobrino A, Bueno-Beti C, Tarin JJ, Monsalve E, Sanchis J and Hermenegildo C. Estradiol, acting through estrogen receptor alpha, restores dimethylarginine dimethylaminohydrolase activity and nitric oxide production in oxLDL-treated human arterial endothelial cells. Mol Cell Endocrinol 2013; 365: 11-16.

[4] Jung CH, Lee WJ, Hwang JY, Lee MJ, Seol SM, Kim YM, Lee YL, Kim HS, Kim MS and Park JY. Vaspin increases nitric oxide bioavailability through the reduction of asymmetric dimethylarginine in vascular endothelial cells. PLoS One 2012; 7: e52346.

[5] Antoniades C, Bakogiannis C, Tousoulis D, Antonopoulos AS and Stefanadis C. The CD40/CD40 ligand system: linking inflammation with atherothrombosis. J Am Coll Cardiol 2009; 54: 669-677.

[6] Bhogal RH, Weston CJ, Curbishley SM, Adams DH and Afford SC. Activation of CD40 with platelet derived CD154 promotes reactive oxygen species dependent death of human hepatocytes during hypoxia and reoxygenation. PLoS One 2012; 7: e30867.

[7] Hausding M, Jurk K, Daub S, Kroller-Schon S, Stein J, Schwenk M, Oelze M, Mikhed Y, Kerahrodi JG, Kossmann S, Jansen T, Schulz E, Wenzel P, Reske-Kunz AB, Becker C, Munzel T, Grabbe S and Daiber A. CD40L contributes to angiotensin II-induced pro-thrombotic state, vascular inflammation, oxidative stress and endothelial dysfunction. Basic Res Cardiol 2013; 108: 386.

[8] Bou KL, Hachem A, Zaid Y, Boulahya R, Mourad W and Merhi Y. Soluble CD40 ligand impairs the anti-platelet function of peripheral blood angiogenic outgrowth cells via increased production of reactive oxygen species. Thromb Haemost 2013; 109: 940-947.

[9] Meltzer PS. Cancer genomics: small RNAs with big impacts. Nature 2005; 435: 745-746.

[10] Pang H, Zheng Y, Zhao Y, Xiu X and Wang J. miR-590-3p suppresses cancer cell migration, invasion and epithelial-mesenchymal transition in glioblastoma multiforme by targeting ZEB1 and ZEB2. Biochem Biophys Res Commun 2015; 468: 739-745.

[11] Bao MH, Li JM, Zhou QL, Li GY, Zeng J, Zhao J and Zhang YW. Effects of miR590 on oxLDL induced endothelial cell apoptosis: roles of p53 and NFkappaB. Mol Med Rep 2016; 13: 867-873.

[12] Luo P, Zhang WF, Qian ZX, Xiao LF, Wang H, Zhu TT, Li F, Hu CP and Zhang Z. MiR-590-5p-meidated LOX-1 upregulation promotes angiotensin II-induced endothelial cell apoptosis. Biochem Biophys Res Commun 2016; 471: 402-408.

[13] Dai Y, Zhang Z, Cao Y, Mehta JL and Li J. MiR-590-5p Inhibits oxidized- LDL induced angiogenesis by targeting LOX-1. Sci Rep 2016; 6: 22607.

[14] Shakibaei M, Kraehe P, Popper B, Shayan P, Goel A and Buhrmann C. Curcumin potentiates antitumor activity of 5-fluorouracil in a 3D alginate tumor microenvironment of colorectal cancer. Bmc Cancer 2015; 15: 250.

[15] Ferreira VH, Nazli A, Dizzell SE, Mueller K and Kaushic C. The anti-inflammatory activity of curcumin protects the genital mucosal epithelial barrier from disruption and blocks replication of HIV-1 and HSV-2. PLoS One 2015; 10: e124903.

[16] Das L and Vinayak M. Long term effect of curcumin in restoration of tumour suppressor p53 and phase-II antioxidant enzymes via activation of Nrf2 signalling and modulation of in-

flammation in prevention of cancer. PLoS One 2015; 10: e124000.
[17] Pan Y, Wang Y, Zhao Y, Peng K, Li W, Wang Y, Zhang J, Zhou S, Liu Q, Li X, Cai L and Liang G. Inhibition of JNK phosphorylation by a novel curcumin analog prevents high glucose-induced inflammation and apoptosis in cardiomyocytes and the development of diabetic cardiomyopathy. Diabetes 2014; 63: 3497-3511.
[18] Qiao Q, Jiang Y and Li G. Inhibition of the PI3K/AKT-NF-kappaB pathway with curcumin enhanced radiation-induced apoptosis in human Burkitt's lymphoma. J Pharmacol Sci 2013; 121: 247-256.
[19] Masuelli L, Benvenuto M, Fantini M, Marzocchella L, Sacchetti P, Di Stefano E, Tresoldi I, Izzi V, Bernardini R, Palumbo C, Mattei M, Lista F, Galvano F, Modesti A and Bei R. Curcumin induces apoptosis in breast cancer cell lines and delays the growth of mammary tumors in neu transgenic mice. J Biol Regul Homeost Agents 2013; 27: 105-119.
[20] Bounaama A, Djerdjouri B, Laroche-Clary A, Le Morvan V and Robert J. Short curcumin treatment modulates oxidative stress, arginase activity, aberrant crypt foci, and TGF-beta1 and HES-1 transcripts in 1,2-dimethylhydrazine-colon carcinogenesis in mice. Toxicology 2012; 302: 308-317.
[21] Kim YS, Ahn Y, Hong MH, Joo SY, Kim KH, Sohn IS, Park HW, Hong YJ, Kim JH, Kim W, Jeong MH, Cho JG, Park JC and Kang JC. Curcumin attenuates inflammatory responses of TNF-alpha-stimulated human endothelial cells. J Cardiovasc Pharmacol 2007; 50: 41-49.
[22] Kunwittaya S, Treeratanapiboon L, Srisarin A, Isarankura-Na-Ayudhya C and Prachayasittikul V. In vitro study of parasite elimination and endothelial protection by curcumin: adjunctive therapy for cerebral malaria. Excli J 2014; 13: 287-299.
[23] Yamamoto E, Hirata Y, Tokitsu T, Kusaka H, Sakamoto K, Yamamuro M, Kaikita K, Watanabe H, Hokimoto S, Sugiyama S, Maruyama T and Ogawa H. The pivotal role of eNOS uncoupling in vascular endothelial dysfunction in patients with heart failure with preserved ejection fraction. Int J Cardiol 2015; 190: 335-337.
[24] Li Q, Atochin D, Kashiwagi S, Earle J, Wang A, Mandeville E, Hayakawa K, D'Uscio LV, Lo EH, Katusic Z, Sessa W and Huang PL. Deficient eNOS phosphorylation is a mechanism for diabetic vascular dysfunction contributing to increased stroke size. Stroke 2013; 44: 3183-3188.
[25] Sharma A, Sellers S, Stefanovic N, Leung C, Tan SM, Huet O, Granville DJ, Cooper ME, de Haan JB and Bernatchez P. Direct eNOS activation provides atheroprotection in diabetes-accelerated atherosclerosis. Diabetes 2015; 64: 3937-3950.
[26] Su Y, Qadri SM, Hossain M, Wu L and Liu L. Uncoupling of eNOS contributes to redox-sensitive leukocyte recruitment and microvascular leakage elicited by methylglyoxal. Biochem Pharmacol 2013; 86: 1762-1774.
[27] Schonbeck U and Libby P. The CD40/CD154 receptor/ligand dyad. Cell Mol Life Sci 2001; 58: 4-43.
[28] Aukrust P, Damas JK and Solum NO. Soluble CD40 ligand and platelets: self-perpetuating pathogenic loop in thrombosis and inflammation? J Am Coll Cardiol 2004; 43: 2326-2328.
[29] Ma Y, Chen Z, Zou Y and Ge J. Atorvastatin represses the angiotensin 2-induced oxidative stress and inflammatory response in dendritic cells via the PI3K/Akt/Nrf 2 pathway. Oxid Med Cell Longev 2014; 2014: 148798.
[30] Zhang B, Wu T, Song C, Chen M, Li H and Guo R. Association of CD40--1C/T polymorphism with cerebral infarction susceptibility and its effect on sCD40L in Chinese population. Int Immunopharmacol 2013; 16: 461-465.
[31] Zhang B, Wu T, Chen M, Zhou Y, Yi D and Guo R. The CD40/CD40L system: a new therapeutic target for disease. Immunol Lett 2013; 153: 58-61.
[32] Zhang B, Chen M, Yang H, Wu T, Song C and Guo R. Evidence for involvement of the CD40/CD40L system in post-stroke epilepsy. Neurosci Lett 2014; 567: 6-10.
[33] Guo X, Yu L, Chen M, Wu T, Peng X, Guo R and Zhang B. miR-145 mediated the role of aspirin in resisting VSMCs proliferation and anti-inflammation through CD40. J Transl Med 2016; 14: 211.
[34] Sharma S, Chopra K, Kulkarni SK and Agrewala JN. Resveratrol and curcumin suppress immune response through CD28/CTLA-4 and CD80 co-stimulatory pathway. Clin Exp Immunol 2007; 147: 155-163.
[35] Duan W, Yang Y, Yan J, Yu S, Liu J, Zhou J, Zhang J, Jin Z and Yi D. The effects of curcumin post-treatment against myocardial ischemia and reperfusion by activation of the JAK2/STAT3 signaling pathway. Basic Res Cardiol 2012; 107: 263.
[36] Soetikno V, Sari FR, Sukumaran V, Lakshmanan AP, Mito S, Harima M, Thandavarayan RA, Suzuki K, Nagata M, Takagi R and Watanabe K. Curcumin prevents diabetic cardiomyopathy in streptozotocin-induced diabetic rats: possible involvement of PKC-MAPK signaling pathway. Eur J Pharm Sci 2012; 47: 604-614.
[37] Li X, Lu Y, Sun Y and Zhang Q. Effect of curcumin on permeability of coronary artery and

expression of related proteins in rat coronary atherosclerosis heart disease model. Int J Clin Exp Pathol 2015; 8: 7247-7253.

[38] Reuter S, Charlet J, Juncker T, Teiten MH, Dicato M and Diederich M. Effect of curcumin on nuclear factor kappaB signaling pathways in human chronic myelogenous K562 leukemia cells. Ann N Y Acad Sci 2009; 1171: 436-447.

[39] Wu J, Yang X, Zhang YF, Zhou SF, Zhang R, Dong XQ, Fan JJ, Liu M and Yu XQ. Angiotensin II upregulates Toll-like receptor 4 and enhances lipopolysaccharide-induced CD40 expression in rat peritoneal mesothelial cells. Inflamm Res 2009; 58: 473-482.